Transport of biochar colloids in saturated porous media in the presence of humic substances or proteins

Article · December 2018

DOI: 10.1016/j.envpol.2018.12.075

CITATIONS
0

READS
66

6 authors, including:

Yang Wang
China Agricultural University
3 PUBLICATIONS **11** CITATIONS
SEE PROFILE

Prabhakar Sharma
Nalanda University
48 PUBLICATIONS **301** CITATIONS
SEE PROFILE

Jianying Shang
China Agricultural University
23 PUBLICATIONS **80** CITATIONS
SEE PROFILE

Environmental Pollution 246 (2019) 855–863

Contents lists available at ScienceDirect

Environmental Pollution

journal homepage: www.elsevier.com/locate/envpol

Transport of biochar colloids in saturated porous media in the presence of humic substances or proteins☆

Wen Yang [a], Scott A. Bradford [b], Yang Wang [a], Prabhakar Sharma [c], Jianying Shang [a, *], Baoguo Li [a]

[a] College of Resources and Environmental Sciences, China Agricultural University, Key Laboratory of Plant-Soil Interactions, The Ministry of Education, Key Laboratory of Arable Land Conservation in North China, The Ministry of Agriculture, Beijing, 100193, China
[b] US Salinity Laboratory, USDA, ARS, Riverside, CA, 92507, United States
[c] School of Ecology and Environment Studies, Nalanda University, Rajgir, Nalanda, Bihar, India

ARTICLE INFO

Article history:
Received 12 October 2018
Received in revised form
3 December 2018
Accepted 23 December 2018
Available online 28 December 2018

Keywords:
Colloidal biochar particle
Dissolved organic matter
Humic acid
Protein

ABSTRACT

Application of biochar in the field has received considerable attention in recent years, but there is still little known about the fate and transport of biochar colloids (BCs) in the subsurface. Natural organic matter (NOM), which mainly consists of humic substance (HS) and proteins, is ubiquitous in the natural environment and its dissolved fraction is active and mobile. In this study, the transport of BCs in saturated porous media has been examined in the presence of two HS (humic and fulvic acids) and two proteins. Bull serum albumin (BSA) and Cytochrome *c* (Cyt) were selected to present the negatively and positively charged protein, respectively. At low and high salt concentration and different pH conditions, the transport of BCs was strongly promoted by HS. HS significantly increased the mobility of BCs in porous media under both low and high salt conditions due to the enhanced electrostatic repulsion and modification of surface roughness and charge heterogeneity. While BC mobility in porous media was suppressed by both BSA and Cyt in the low salt solution, the presence of BSA largely promoted and Cyt slightly enhanced the transport of BCs in high salt solutions. BSA and Cyt adsorption onto BC surface decreased the negative charge of BC and resulted in a less repulsive interaction in low salt solutions. In high salt solutions, the adsorbed BSA layers disaggregated BCs and reduced the strength of the interaction between BC and the sand. Adsorbed Cyt on BCs caused more attractive patches between BC and sand surface, and greater retention than BSA.

1. Introduction

Biochar is a type of black carbon derived from low-temperature (<700 °C) pyrolysis of biomass (Lehmann et al., 2006, Lehmann, 2007a; Lehmann and Joseph, 2015). In recent years, biochar has been widely applied into soils to sequester carbon and mitigate atmospheric carbon dioxide, improve soil quality and structure, encourage microbial activity, increase crop production, and immobilize pollutants, such as heavy metals, polycyclic aromatic hydrocarbons (PAHs), pesticides, and microbial pathogens (Lehmann, 2007b; Lehmann et al., 2011; Qian et al., 2016; Yavari et al., 2015). Conversely, relatively little is known about potential risks from mobile biochar particles in the field, such as colloid-facilitated contaminant transport (Zhang et al., 2010). Knowledge related to biochar particle mobility and fate in the subsurface under natural environmental conditions is therefore important for advancing the science behind field biochar application and evaluating the potential long-term risks (Wang et al., 2013a).

Several studies about the transport and retention of biochar particles in the subsurface have been investigated at the laboratory and field scales (Chen et al., 2017; Dittmar et al., 2012; Obia et al., 2017; Wang et al., 2013a; Yang et al., 2017a; Zhang et al., 2010). When the solution chemistry had the low ionic strength (IS) or high pH, fine biochar particles were easily transported with saturated water flow in porous media (Chen et al., 2017; Zhang et al., 2010). Biochar particles derived from lower pyrolysis temperatures and with smaller sizes exhibited greater mobility in porous media (Wang et al., 2013a). Furthermore, chemical heterogeneity played an insignificant role in the retention of nano-sized biochar particles

☆ This paper has been recommended for acceptance by Dr. Yong Sik Ok.
* Corresponding author.
E-mail address: jyshang@cau.edu.cn (J. Shang).

https://doi.org/10.1016/j.envpol.2018.12.075
0269-7491/

(Wang et al., 2013a). Black carbon mobility in dissolved (less than 0.45 μm) and colloidal phase is an important pathway of black carbon export from the subsurface (Guggenberger et al., 2008; Hockaday et al., 2007) and catchments (Dittmar et al., 2012). To date, few published studies have reported on the influence of dissolved organic matter (DOM) on the stability, transport, and retention of BCs. DOM is commonly found in natural aquatic and soil environments (Nebbioso and Piccolo, 2013). Humic-like and protein-like substances are two major components of DOM (Burdige et al., 2004). Humic substances (HS) are derived from the degradation of organic matter and are usually categorized into three groups: humic acid (HA), fulvic acid (FA), and humin (Jones and Bryan, 1998; Piccolo, 2001). Proteins are major components of extracellular macromolecules (e.g., biopolymers) that are produced by microorganisms and are found on their surfaces (More et al., 2014). The presence or adsorption of HS and proteins on surfaces can have a large influence on the stability, transport, and retention of colloids and nanoparticles in porous media (Franchi and O'Melia, 2003; Furukawa et al., 2009; Kretzschmar et al., 1995; Lin et al., 2017; Liu et al., 2007; Philippe and Schaumann, 2014; Sheng et al., 2016; Sun et al., 2016; Yang et al., 2013).

Interestingly, the presence of DOM has been reported to either favor colloid mobility (Jones and Su, 2014; Yang et al., 2013; Yuan et al., 2008) or enhance retention (Espinasse et al., 2007; Xiao and Wiesner, 2013; Yang et al., 2012b). There might be the complex interaction between colloids and DOM. For example, DOM has been reported to change colloid and nanoparticle mobility by competing for the same retention sites on the porous media (Liang et al., 2013; Wu et al., 2018), masking charge heterogeneity (Wang et al., 2015), inducing larger electrostatic (Wang et al., 2013b) or electrosteric repulsion (Jung et al., 2014; Wu et al., 2018), and altering the surface roughness (Jones and Su, 2014; Zhang et al., 2016). HA and FA generally enhanced the transport of colloids and nanoparticles in porous media (Jones and Su, 2014; Morales et al., 2011; Wang et al., 2013b; Yang et al., 2012a). Conversely, proteins coating on the sand surface diminished colloid transport and enhance retention through hydrophobic interactions (He et al., 2015; Xiao and Wiesner, 2013). Narvekar et al. (2017) found that extracellular polymeric substances (EPS) attached to the surface of hematite nanoparticles (HNP) and decreased HNP retention in porous media. Wu et al. (2018) found that positively charged trypsin inhibited bacteria mobility in quartz sand while negatively charged BSA increased the transport of bacteria. Consequently, different DOM components are likely to produce a dissimilar effect on colloid transport and retention in a porous medium under varying solution chemistry conditions (Philippe and Schaumann, 2014). An improved understanding of the influence of DOM on BC transport under varying solution chemistry conditions is therefore crucial to elucidate the mobility and fate of BCs under natural conditions and to assess the long-term risk of biochar-field application.

The objective of this study was to examine the effects of HS and protein on the stability, transport, and retention of BCs in saturated porous media under various solution pH and ionic strength (IS) conditions. In this research, BC surface charge, aggregation behavior, column breakthrough curves under different DOM and solution chemistry conditions, and the interaction energies between BC and porous media were investigated to provide valuable insight on the influence of different DOM and solution chemistry conditions on BC transport and retention in saturated porous media.

2. Materials and methods

2.1. DOM

Suwannee River humic acid (SRHA, 2S101H, International Humic Substances Society) and Suwannee River fulvic acid (SRFA, 2S101F, International Humic Substances Society) were used as representative HS. In this study, Bull Serum Albumin (BSA, A7030, Sigma) and Cytochrome *c* from bovine heart (Cyt, C2037, Sigma) were used as the typical proteins commonly found in natural environments. BSA and Cyt are less water soluble globular proteins, which are ubiquitous in nature (Furkan et al., 2017; Huangfu et al., 2013; Sheng et al., 2016). These four DOM stock suspensions were all passed through a 0.45 μm filter (Jinlong Nylon Membrane Filters, Tianjin, CN). The concentration of each filtrate was determined from a mass balance after drying a sample suspension volume and then weighing the residue. All the stock solutions were stored in the dark at 4 °C until use.

2.2. Characteristics of biochar particles

The biochar used in this study was derived from pyrolyzing wheat straw (Zhengzhou, Henan Province, CN) at 600 °C for 1 h under limited oxygen conditions. The resultant biochar sample was allowed to cool at room temperature, and then a ball mill was used to grind it into powder form with a colloidal size range of 200–900 nm. This biochar powder (0.5 g) was added into 50 mL of deionized (DI) water to create a stock suspension and sonicated in a water bath for 10 min before use.

The elemental content of the biochar including carbon (C), hydrogen (H), nitrogen (N), and sulphur (S) was determined with an Elemental analyzer (Flash 2000, Thermo Scientific, USA). The functional groups of biochar were analyzed using Fourier Transform Infrared spectroscopy (FTIR, Spectrum Spotlight 200 FT-IR microscopy, PE, USA). The sessile drop method was used to analyze the static contact angles of the biochar using a goniometer (JC2000D2, Powereach, CN). A Transmission Electron Microscope (TEM, JEOL JEM-1230, JPN) was used to study the morphology of BCs. A 50 mg L^{-1} BCs suspension was prepared in the absence/presence of 5 mg L^{-1} carbon concentration of DOM. The hydrodynamic diameter and electrophoretic mobility of bare BCs and DOM-coated BCs (DOM-BCs) were measured using a Zetasizer (Nano ZS90, Malvern, UK) under various solution chemistry conditions by adding 0.01 M HCl or NaOH solution and concentrated NaCl solution. All the experimental treatments are shown in detail in Table 1. For every sample measurement, at least three independent tests with no less than 15 cycles for each run were conducted. The colloidal stability of BCs was evaluated by examining the sedimentation profile of the particle suspensions under 10 mM NaCl (pH 7) and 1 mM NaCl (pH 5, 7, and 10) conditions, respectively. More details can be found in the supporting information (S1).

Experiments were performed to determine the adsorption of different DOM onto BCs (see section S2 in the supporting information). Electrophoretic mobilities (EPM) of BCs in the presence of DOM at three pH conditions were interpreted using Ohshima's soft particle theory (Nakamura et al., 1992; Ohshima et al., 1992; Phenrat et al., 2010) which is summarized in Eqs. S1-S5 of the supplementary material. A nonlinear least square optimization algorithm (i.e., trust-region reflective Newton) with MATLAB (Natick, MA) was used to iteratively fit the EPM data using appropriate initial parameter values to obtain realistic estimates for three unknown parameters of Ohshima's theory, i.e., charge density (ZN/N_A), layer thickness (d), and softness parameter ($1/\lambda$) (Phenrat et al., 2010).

2.3. Porous medium

Quartz sand (grain size 0.425–0.600 mm, Sinopharm, China) was used as the porous medium in column experiments. To remove metal oxides, the sand was soaked in concentrated HCl solution for

Table 1
Electrokinetic potentials of BCs and quartz sands, DLS size for BC, mass percentages of the BCs recovered from column experiment, and fitted parameters for breakthrough curves using two-site kinetic retention model under various solution chemistry conditions.

IS (mM)	pH	DOM type	ζ_{BC} [a] (mV)	ζ_s [b] (mV)	DLS size [c] (nm)	M_{eff} [d] (%)	M_{ret} [e] (%)	M_{tot} [f] (%)	k_{att} [g] (min^{-1})	k_{det} [h] (min^{-1})	k_{str} [i] (min^{-1})	R^2
1	7	–	−51.06 ± 1.16	−51.77 ± 0.75	707 ± 70	52.1	39.9	92.0	6.77×10^{-3}	8.09×10^{-4}	0.094	0.993
1	7	HA	−53.60 ± 0.28	−55.13 ± 1.52	725 ± 14	57.8	35.4	93.2	2.07×10^{-3}	4.68×10^{-3}	0.094	0.988
1	7	FA	−52.33 ± 0.64	−52.93 ± 1.75	737 ± 43	57.0	36.3	93.3	3.66×10^{-3}	1.38×10^{-3}	0.094	0.992
1	7	BSA	−41.07 ± 0.71	−37.37 ± 1.93	771 ± 65	31.2	66.1	97.4	2.88×10^{-2}	2.83×10^{-4}	0.094	0.993
1	7	Cyt	−18.87 ± 0.60	−36.03 ± 1.77	1071 ± 58	11.8	75.0	86.8	3.62×10^{-2}	2.47×10^{-4}	0.206	0.982
1	5	–	−40.25 ± 1.37	−36.30 ± 1.41	783 ± 95	30.3	65.9	96.2	3.47×10^{-2}	6.15×10^{-4}	0.105	0.979
1	5	HA	−47.37 ± 0.93	−37.43 ± 1.25	782 ± 53	33.4	51.9	85.3	2.45×10^{-2}	1.05×10^{-3}	0.102	0.986
1	5	FA	−49.70 ± 0.28	−44.43 ± 1.78	724 ± 56	44.1	43.8	87.9	1.56×10^{-2}	1.29×10^{-3}	0.101	0.964
1	5	BSA	−31.37 ± 0.35	−25.80 ± 0.30	1095 ± 78	7.7	76.9	84.6	5.58×10^{-2}	2.83×10^{-5}	0.165	0.994
1	5	Cyt	−16.10 ± 0.60	−16.30 ± 0.10	1226 ± 89	3.1	84.7	87.8	6.15×10^{-2}	2.49×10^{-5}	0.312	0.979
1	10	–	−51.39 ± 0.75	−60.10 ± 1.71	693 ± 21	54.0	34.4	88.5	7.57×10^{-3}	2.75×10^{-3}	0.091	0.997
1	10	HA	−54.47 ± 0.74	−64.00 ± 1.37	632 ± 32	62.2	26.9	89.1	2.81×10^{-3}	3.34×10^{-2}	0.091	0.993
1	10	FA	−52.40 ± 0.50	−61.57 ± 1.01	708 ± 32	59.8	26.5	86.3	3.62×10^{-3}	1.18×10^{-2}	0.090	0.989
1	10	BSA	−48.33 ± 0.06	−49.07 ± 2.14	676 ± 50	42.9	50.3	93.2	1.40×10^{-2}	8.33×10^{-4}	0.091	0.993
1	10	Cyt	−24.37 ± 0.40	−41.80 ± 0.67	831 ± 103	36.9	45.3	82.2	5.31×10^{-3}	2.14×10^{-4}	0.159	0.990
10	7	–	−42.07 ± 0.67	−38.50 ± 1.47	1085 ± 91	6.6	85.0	91.6	6.32×10^{-2}	3.45×10^{-4}	0.236	0.999
10	7	HA	−52.63 ± 0.61	−42.90 ± 1.35	797 ± 47	40.6	48.7	89.3	1.15×10^{-2}	4.15×10^{-4}	0.111	0.987
10	7	FA	−48.30 ± 0.61	−41.63 ± 0.81	825 ± 57	35.8	53.0	88.8	1.85×10^{-2}	3.95×10^{-4}	0.116	0.986
10	7	BSA	−37.73 ± 2.47	−36.07 ± 1.07	727 ± 44	54.1	33.5	87.7	6.80×10^{-3}	2.82×10^{-4}	0.099	0.980
10	7	Cyt	−17.80 ± 0.10	−31.90 ± 1.31	1128 ± 32	7.6	83.8	91.4	4.76×10^{-2}	7.27×10^{-6}	0.216	0.926

[a,b] ζ-potentials ± standard deviation (triplicate experiments) of BCs and quartz sands, respectively. [c] Mean size ± standard deviation (triplicate experiments) of BCs. [d,e,f] Effluent, retained, and total percentages of the BCs recovered from column experiment. [g,h] First-order attachment and detachment coefficients on reversible kinetic retention site 1, respectively. [i] First-order retention coefficient on irreversible kinetic retention site 2.

24 h, and then thoroughly washed with DI water. After that, the sand was dried at 105 °C for 8 h and baked at 600 °C for 4 h in a muffle furnace for removing organic matter (Tian et al., 2015). The cleaned sand was stored in PTFE plastic bottles until use. The ζ-potential of the sand under various solution chemistry conditions was determined using the following procedure: the sand was ground into powder and added to an electrolyte solution, the sand suspension was allowed to settle, and then the ζ-potential of the supernatant was measured using the Zetasizer.

2.4. Column experiments

Electrolyte solutions with selected NaCl concentrations and pH were prepared (Table 1). The pH and IS of the injection suspensions were adjusted by adding 0.01 M HCl or NaOH and NaCl solutions to obtain three pH (5, 7, and 10) and two IS (1 and 10 mM) solution conditions. A 50 mg L^{-1} BC (C_0) suspension was prepared in a selected electrolyte solution.

Column experiments were performed in a stainless steel column with 2.5 cm inner diameter and 12 cm length. The column was wet-packed with clean quartz sand that was added in 2 cm intervals. The average bulk density of the packed column was 1.41 g cm^{-3}, and the average porosity was 0.47. The column experiments were run in an upward mode using a peristaltic pump, and BC suspension was injected at a pore water velocity of 26 cm h^{-1}. More than 5 pore volumes (PVs) of background electrolyte solution were introduced into the column to achieve steady flow and chemical equilibrium conditions. The BC suspension was then injected into the column for 3 PVs in the presence/absence of 5 mg C L^{-1} DOM (including HA, FA, BSA, and Cyt) (Table 1). The experiments were continued by injection of 5 PVs of biochar and DOM free background electrolyte solution to flush the mobile BCs out of the column. The column effluents were collected at every 5 min using a fraction collector (Huxi, Shanghai, China). The concentration of BC in effluent samples was measured using a UV-VIS spectrophotometer at a wavelength of 790 nm (Yang et al., 2017b).

After recovery of the BC breakthrough curve (BTC), the column was carefully sectioned into 12 layers of approximately 1-cm segments to determine the spatial distribution of retained BCs. The excavated quartz sands were placed into a 50-mL glass flask with 20 mL of DI water, and shaken at 120 rpm for 4 h. The concentration of BCs in the suspensions was determined using the spectrophotometric method and the biochar recoveries of the whole column experiments were calculated as a function of depth. The initial injected BC amount, the masses of BC in the effluent, and retained BC in the sands were compared to obtain the mass balance.

Conservative tracer (3 mM $NaNO_3$) experiments were conducted in a similar manner to the BC BTC studies. In brief, 5 PVs of DI water were injected into the column, followed by 3 PVs of 3 mM $NaNO_3$ solution, and then 5 PVs of DI water. The concentration of $NaNO_3$ in the effluents was determined using UV-VIS spectrophotometer and calibration curve at a wavelength of 235 nm (Shang et al., 2010). The dispersivity was obtained by fitting $NaNO_3$ BTC using the one-dimensional convection-dispersion equation in the HYDRUS-1D software (Šimunek et al., 1998). This software was also used to simulate BC transport and retention in porous media under the various solution chemistry conditions (see section S4 in the supporting information). Two kinetic retention sites were employed, one which considered first-order attachment and detachment, and the other irreversible, depth-dependent retention.

3. Results and discussion

3.1. Characteristics of biochar and DOM

The TEM image of BCs in Fig. 1 shows that the morphology consists of an irregular shape and rough surface. The average hydrodynamic size of BCs was determined to be 457.2 ± 110.6 nm by the DLS method (Fig. S1). The chemical composition of the wheat straw-derived biochar was C (60.2%), H (1.6%), O (37.2%), N (0.5%), and S (0.5%), and the FTIR spectra of the biochar (Fig. S2) showed

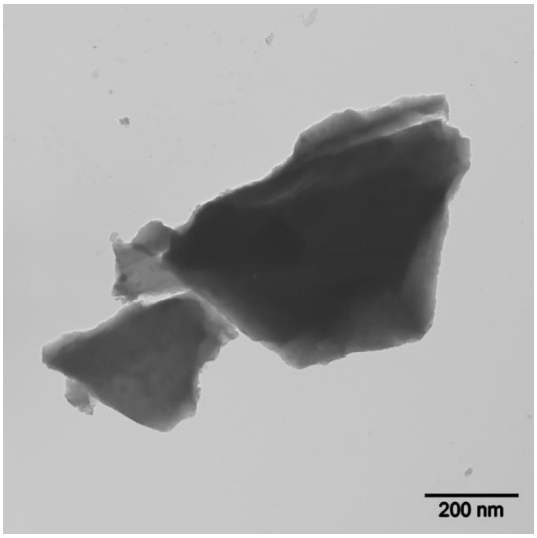

Fig. 1. TEM image of BCs.

the presence of –COOH, C–H in-plane, –OH, C–O, and aromatic C=C and C–H functional groups (Yang et al., 2017b). Fig. 2 shows that the ζ-potential of bare BCs (absence of DOM) varied from −29.9 mV at pH 4 to −51.4 mV at pH 10 in 1 mM NaCl solution due to deprotonation of surface functional groups. An increase in IS from 1 to 10 mM NaCl at pH = 7 produced an increase in ζ-potential for bare BCs from −51.1 mV to −42.1 mV (Table 1) due to the influence of counter ions. The contact angles of BCs were 122.6 ± 3.0°, 99.7 ± 8.4°, and 0° in the presence of water, glycerinum, and n-decane, respectively (Yang et al., 2017b). The biochar material was therefore considered to be hydrophobic, and Lewis acid-base interactions were included in the interaction energy calculations discussed below.

3.2. Biochar colloid properties in presence of DOM

The HA, FA, BSA, and Cyt properties are shown in Table S1, and the ζ-potential plots of HA, FA, BSA, and Cyt in 1 mM NaCl solution as pH varying from 4 to 10 was presented in Fig. S3. The HA, FA, and BSA showed negative ζ-potentials with the absolute value trend (BSA < FA < HA) at a given pH, and Cyt was positively charged under most pH conditions. Other studies also showed that the ζ-potentials of HA were −20 mV at pH 3.5 and −44 mV at pH 10 (Mohd Omar et al., 2014), the ζ-potentials of FA were −35 mV at pH 2 and -60 mV at pH 10 (Palomino and Stoll, 2013), and the points of Cyt and BSA zero charge were around 10.4 and 4.7 (Salgin et al., 2012; Sheng et al., 2016).

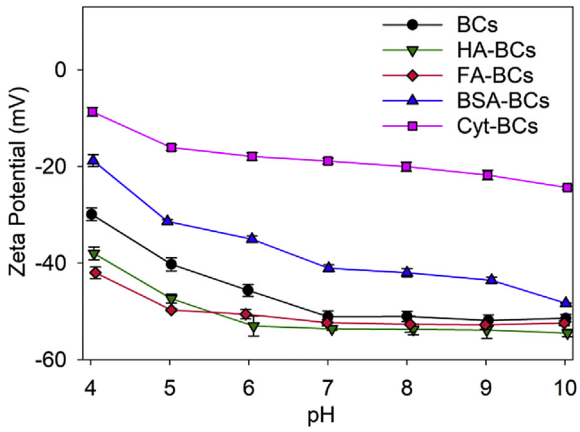

Fig. 2. ζ-potential variation of BCs without/with HA, FA, BSA, and Cyt as a function of pH in 1 mM NaCl solution.

The ζ-potentials and hydrodynamic diameters of BCs in the absence/presence of DOM under varying solution chemistry conditions are presented in Fig. 2, S4 and Table 1. Compared to the bare BC (from −29.9 mV at pH 4 to −51.4 mV at pH 10), the BCs showed more negative surface charge under FA coating (from −42.0 mV at pH 4 to −52.4 mV at pH 10) and HA coating (from −38.0 mV at pH 4 to −54.5 mV at pH 10). Other researchers have also reported that adsorption of HA and FA onto the surface of particles increased their negative charge (Dong et al., 2016; Wang et al., 2013b; Zhang et al., 2013). In contrast, the BCs showed less negative apparent surface charge when BSA (from −18.8 mV at pH 4 to −48.3 mV at pH 10) and Cyt (from −8.7 mV at pH 4 to −24.4 mV at pH 10) were adsorbed on its surface, because bare BC was more negatively charged than BSA and Cyt (Fig. S3). The negative charge density on the surface of multi-walled carbon nanotubes after coated BSA was similarly found to decrease over pH 4 to 11 (Bozgeyik and Kopac, 2016). When the solution IS was increased from 1 mM to 10 mM, the negative ζ-potentials of BCs in the absence and presence of DOM decreased significantly and slightly, respectively (Table 1). One potential explanation is that adsorbed long-chain DOM reduced the compression of the double layer when the salt concentration became high. HA coating also resulted in a minor decrease in the ζ-potential of polyvinylpyrrolidone-coated Ag nanoparticle (PVP–AgNP) when the IS was increased from 0.5 to 5 mM (Wang et al., 2015). In another study, the presence of NOM weakened the decrease in the absolute value of the negative surface charge on C_{60} nanoparticles when the salt concentration increased from 100 to 500 mM (Shen et al., 2015). The ζ-potential of MnO_2 colloids with BSA coating similarly showed less decrease than that of bare MnO_2 colloids when the $NaNO_3$ solution concentration increased from 10 to 500 mM (Huangfu et al., 2013).

The hydrodynamic diameter of BC with/without DOM tended to decrease with an increase in solution pH (Fig. S4) because a more negative surface charge induced larger electrostatic repulsion (Table 1). The hydrodynamic diameters of BCs in the presence of HA and FA were only slightly different (ranging from 632 to 783 nm) because the ζ-potentials were similar. In contrast, the hydrodynamic diameter of BCs with BSA significantly varied from 1313 nm at pH 4–676 nm at pH 10, and that with Cyt from 1554 nm at pH 4–831 nm at pH 10. These differences were related to the less negative ζ-potentials of BSA and Cyt under acidic and neutral conditions which induced less repulsive electrostatic interaction and more aggregation (McKeon and Love, 2008).

3.3. Effect of DOM on BC transport in low salt solution

Fig. 3a presents the BTCs of BCs in the absence/presence of DOM in 1 mM NaCl solution at pH = 7. All the BTCs of BCs gradually reached a plateau, which indicated that the maximum retention capacity of the sand surface was far from filling and may therefore not be the critical factor in these column experiments (He et al., 2015). In comparison to bare BC, the presence of HS slightly promoted BC transport, whereas the mobility of BCs was greatly reduced in the presence of BSA and especially Cyt proteins (Fig. 3a). These trends were generally consistent with the ζ-potentials of BCs in the presence and absence of DOM in Fig. 2, with more negative ζ-potentials producing greater transport. HS have been similarly reported to enhance biochar and ZnO nanoparticles transport in porous media (Jones and Su, 2014; Wang et al., 2013b).

Fig. 3b shows the RPs for BCs with/without DOM in 1 mM NaCl

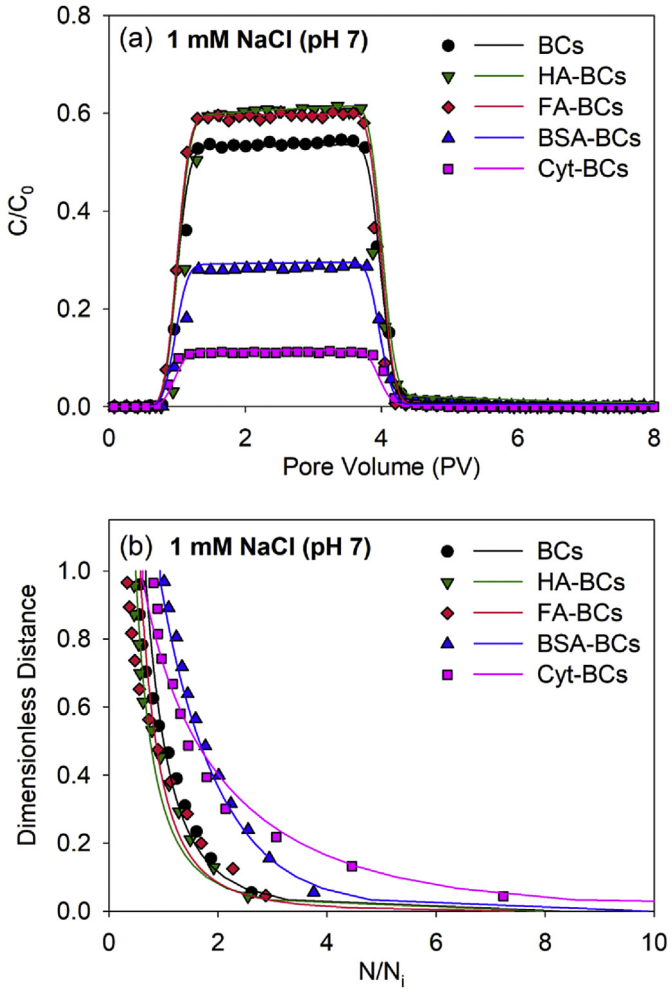

Fig. 3. (a) Measured (symbols) and fitted (lines) breakthrough curves, (b) retention profiles for BCs with/without DOM at 1 mM NaCl and pH 7. The fitted curves were obtained using two-site kinetic retention model. *C*: BCs concentration in the effluents, C_0: injected BCs concentration, Pore volume (PV): the pore volume of the packed column, Dimensionless distance: the distance from column inlet, *N*: residual BCs mass in one pore volume, N_i: BCs mass in one pore volume of the injected BCs suspension.

solution. Consistent with the BTCs, about 35%–75% of the injected BCs were retained on the sand surface (Table 1). The RPs exhibited a hyper-exponential shape (Fig. 3b), which meant that the retention rate of BCs was very high near the column inlet and then decreased rapidly as the depth increased. Wang et al. (2013a) similarly observed a lot of nano- or micro-sized biochar retention and hyper-exponential RPs in saturated porous media under a low IS condition. The total mass balance of BCs was good, ranging from 86.8% to 97.4% (Table 1).

3.4. Effect of DOM for BCs transport in acidic/alkaline solutions

Fig. 4 shows the BTCs and RPs of BCs with/without DOM in acidic (pH = 5) and alkaline (pH = 10) solutions when the IS = 1 mM NaCl. An increase in the solution pH increased the magnitude of the ζ-potential for the BCs and sand and the corresponding repulsive electrostatic interaction (Fig. 2 and Table 1), which produced less BC retention for a given solution chemistry condition (Fig. 3 and Table 1). This behavior agrees well with previous studies on the transport of biochar particles or other types of colloids with increasing pH (Xia et al., 2015; Yang et al., 2017b; Zhang et al., 2010). Less DOM adsorption also occurred on the BCs with increasing pH (Table S2). Similar to Fig. 3 at pH = 7, the presence of HS enhanced and proteins diminished the BC transport in comparison to bare BCs. Specifically, the effluent mass balance of the BTCs (Table 1) followed the trend Cyt < BSA < bare BC < HA < FA at pH = 5, and Cyt < BSA < bare BC < FA < HA at pH = 10. These trends correspond to the measured magnitudes of the ζ-potentials for the BCs (Fig. 2 and Table 1), with less negative (repulsive) ζ-potentials producing greater retention. Note that the effect of FA on biochar mobility was slightly greater than that of HA under acidic conditions due to a more negative surface charge than HA (Table 1). Similar to Fig. 3, RPs for BCs with/without DOM at pH 5 and 10 were also hyper-exponential in shape.

3.5. Effect of DOM on BCs retention in higher salt solution

Fig. 5 shows that the BTCs and RPs of BCs in the absence/presence of DOM in 10 mM NaCl solution at pH = 7. Comparison of Figs. 3 and 5 reveals that an increase in the solution IS from 1 to 10 mM NaCl increased the BC retention (Table 1) due to a decrease in the magnitude of the ζ-potential for the BCs and sand (Table 1), compression of the double layer thickness, and a corresponding decrease in the electrostatic repulsion. Similar results have been observed for studies with biochar particles or other colloids with increasing IS (Cheng et al., 2016; Fang et al., 2013; Rahman et al., 2014; Yang et al., 2017b; Zhang et al., 2010). In addition, greater amounts of DOM adsorption also occurred on BCs with increasing IS (Table S2). HS and proteins always enhanced the transport of BCs at IS = 10 mM NaCl, with the effluent mass balance following the order: bare BC < Cyt < FA < HA < BSA. Note this effluent mass balance order was not consistent with the results at IS = 1 mM and pH = 7 (Fig. 3); i.e., Cyt < BSA < bare BC < FA < HA. Consequently, the adsorbed DOM on the BCs produced a different effect at IS = 1 than at 10 mM NaCl. The effect of BSA on BC transport was much stronger than that of HS, and the reason might be that BSA had larger molecular weight and more BSA was adsorbed on the BCs, which caused the larger thickness of BSA adsorption layer (Table S3). Besides, BSA also caused the small hydrodynamic size of the BCs (Table 1), meaning that BSA inhibited the aggregation process of the BCs in 10 mM NaCl solution. In contrast, Cyt almost did not or slightly facilitated BC transport under 10 mM condition, and one major reason might be that the positively charged Cyt increased the surface charge heterogeneity of the BC surface and induced the attractive patch-charge interaction among BCs, as well as between BC and quartz sand (Sheng et al., 2016; Wu et al., 2018). Various explanations for this difference will be investigated in detail in the next section. Similar to Figs. 3 and 4, RPs for BCs in 10 mM NaCl solution showed a hyper-exponential shape and the presence of HS and BSA except Cyt lessened the retention of the BCs in sands (Fig. 5b).

3.6. Interaction energies and retention mechanisms

Table S4 presents interaction energy parameters between BC and the sand for the various solution chemistry conditions when using Eqs. S10-S13. Results indicate the presence of an insignificant secondary minimum, and a large energy barrier that should inhibit BC retention under all solution chemistry conditions. This finding is obviously not consistent with the experimental observations in Figs. 3–5. Table S5 presents similar interaction energy parameter information when steric interactions were also included using Eqs. S10-S13, S17-S19. The predicted energy barrier is much larger when considering steric interactions than in Table S4. This indicates that inclusion of steric interaction provides an even less plausible explanation for the observed BC retention behavior in Figs. 3–5 than Table S4.

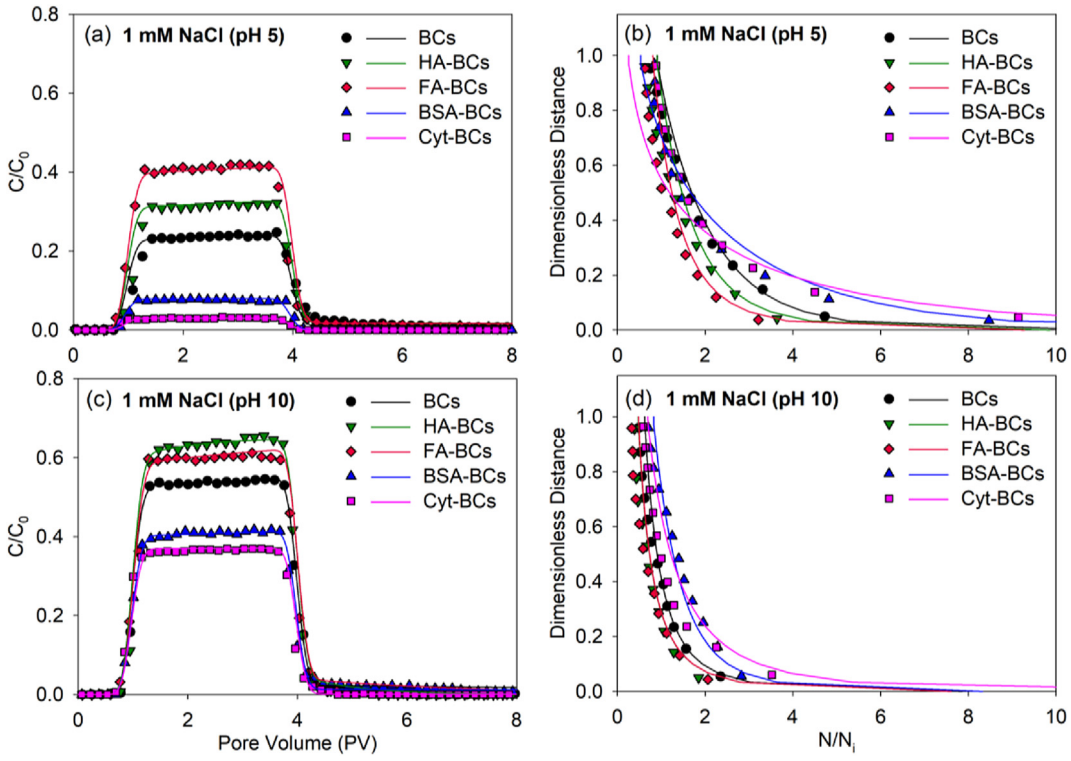

Fig. 4. (a and c) Measured (symbols) and fitted (lines) breakthrough curves and (b and d) retention profiles for BCs in the absence/presence of HA, FA, BSA, and Cyt at 1 mM NaCl solution with (a,b) pH 5 and (c,d) pH 10 conditions.

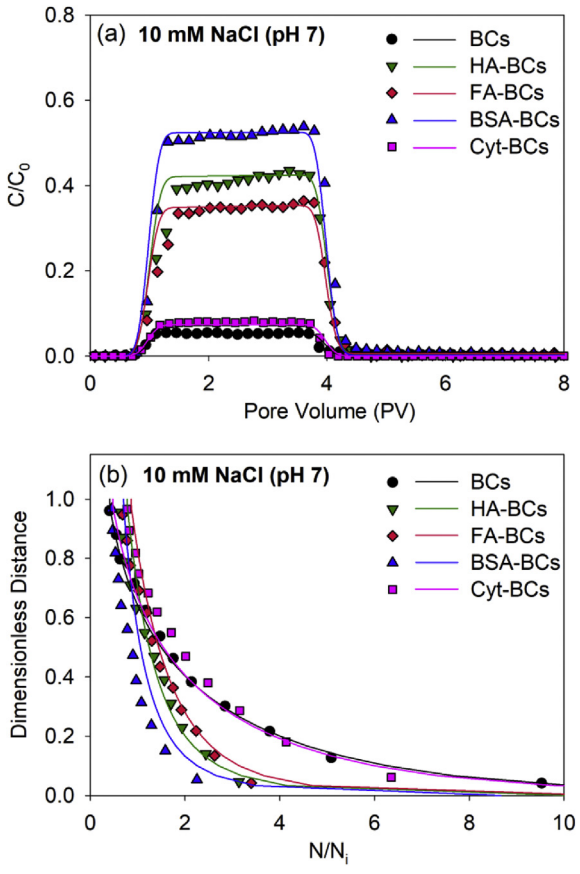

Fig. 5. (a) Measured (symbols) and fitted (lines) breakthrough curves, (b) retention profiles for BCs with/without DOM at 10 mM NaCl solution with pH 7.

Bare BC surfaces exhibit large amounts of roughness in Fig. 1. Adsorbed DOM may also induce nanoscale roughness on the BC surface (Fig. S7). Furthermore, the ζ-potential of the DOM was different from the bare BC (Fig. S3), and this implies that absorbed DOM is expected to induce charge heterogeneity on the surface of the BCs, especially for BSA and Cyt proteins. In addition, nanoscale roughness and chemical heterogeneity are known to be ubiquitous on sand surfaces (Suresh and Walz, 1996; Vaidyanathan and Chi, 1991). Interaction energy parameters have been reported to be very sensitive to nanoscale roughness and chemical heterogeneity parameters (Bendersky and Davis, 2011; Bradford et al., 2017; Bradford and Torkzaban, 2013; Suresh and Walz, 1996). In particular, small fractions of nanoscale roughness have been demonstrated to locally eliminate the energy barrier to produce primary minimum interactions (Bhattacharjee et al., 1998; Hoek and Agarwal, 2006; Huang et al., 2010). The energy barrier height and strength of the primary minimum interaction is a function of the roughness parameters, the solution IS, and the ζ-potential of the surfaces (Kim et al., 2009; Rijnaarts et al., 1999). Shallow primary minima occur when small amounts of nanoscale roughness occur on both interacting surfaces (Bradford et al., 2017; Bradford and Torkzaban, 2013), and colloid interaction in such shallow minima are sometimes subject to diffusive or hydrodynamic removal (Bradford et al., 2017; Bradford and Torkzaban, 2015). Chemical heterogeneity may also lower the energy barrier height and create strong primary minimum interactions on smooth surfaces (Bendersky and Davis, 2011; Bradford and Torkzaban, 2013). Consequently, spatial variability in nanoscale roughness and chemical heterogeneity on the sand and the BC surface provide a viable alternative explanation for BC retention in Figs. 3–5.

The nearly complete recovery of BCs following excavation of the sand into deionized water (82.2–97.4%) indicates that the vast majority of the retained BCs were weakly associated with the sand

surface, even when positively charged Cyt (Fig. S3) was adsorbed onto the BCs (Table S2). This can be explained by alteration of the interaction energy profile by nanoscale roughness on both the sand and the BCs (Bradford et al., 2017). In particular, small amounts of nanoscale roughness have been demonstrated to control the interaction energy profile even in the presence of significant fractions of positive charge heterogeneity (Torkzaban and Bradford, 2016). When colloids are weakly associated with the solid surface, colloid immobilization will be controlled by lever arms arising from deformation and pore space geometry (Torkzaban et al., 2008). The torque balance is always satisfied at a location where the roughness height on the sand is greater than the colloid radius (Rahman et al., 2014; Treumann et al., 2014). Colloid retention at such locations has been referred to as surface straining (Treumann et al., 2014). Strained colloids are released following soil excavation because of the destruction of the pore structure and non-stationary lever arms when the sand continuously mixed (Bradford et al., 2009; Treumann et al., 2014). Furthermore, hyper-exponential RPs (Figs. 3–5) have been associated with straining processes (Bradford et al., 2006, 2007; Sun et al., 2015) and BCs (Wang et al., 2013a, b).

3.7. Mathematical modeling

The BTCs and RPs for BCs in Figs. 3–5 were simulated well ($R^2 > 0.926$) using the transport model with two kinetic retention sites (Table 1 and Figs. 3–5). Most of the BC retention was associated with the irreversible, depth-dependent retention site (>43.2%). The value of k_{str} tended to increase with the hydrodynamic diameter of the BCs, and to be highest in the presence of Cyt due to its larger hydrodynamic diameter and less negative ζ-potential (Table 1). The value of k_{str} was relatively insensitive to the presence and/or absence of other DOM for a given solution chemistry condition. Differences in the retention of bare BCs and in the presence of HA, FA, and BSA for a given solution chemistry were therefore mainly attributed to the retention parameters on the reversible kinetic site. However, detailed interpretation of k_{att} and k_{det} values was hampered by differences in the amount (0.001–56.6%) and reversibility (k_{det} ranged from 7.27×10^{-6} to 3.34×10^{-2} min^{-1}) of retention on this site.

4. Implications

The fate and transport of biomass-derived BCs in a subsurface environment have significant environmental implications for the land application of biochars for carbon sequestration, mitigation of climate change, or soil quality improvement. HS and protein are pervasive and are major fractions of DOM in soil and aquatic environment. This study showed that various DOM ubiquitously present in the environment had a different impact on BC mobility in porous media that depends on the solution chemistry conditions (e.g. pH and IS). This study improved our understanding of the effect of four representative DOMs on BC fate in saturated porous media. If biochar is being applied into the topsoil layer of the agricultural field with a high organic matter, the organic matter might cause more BCs leaching into deeper soil layers following irrigation, rain, and snow melting which may ultimately reduce the long-term effect of biochar application for improving the soil quality. If biochar is added into the soils with animal manure (which usually contains a huge amount of proteins), the negatively/positively charged proteins or the protein mixtures can inhibit the transport of BCs at low ionic strength because of electrostatic repulsion, and the negatively charged proteins can largely improve the stability of the BCs and thus enhanced the mobility of BCs at high ionic strength due to surface alterations. Differential effects of HS and protein suggest that the composition of DOM is an important factor to be considered when assessing the transport, fate and long-term application of biochar in soil and aqueous phase because biochar surface coatings (especially caused by HS and negatively charged protein) can potentially facilitate the mobility of BCs in an environment. The interaction of DOM and biochar should, therefore, be considered before application of a biochar to a particular environment. More intriguingly, it is likely that biomacromolecules (e.g. protein and HS) adsorption onto other colloids and nanoparticles may similarly influence their stability and mobility, and facilitate the transport of associated contaminants under certain environmental conditions.

Acknowledgments

This work was supported by the National Natural Science Foundation of China (41771255, 41501232), the Program of “1000-talents Plan” for young researchers.

Appendix A. Supplementary data

Supplementary data to this article can be found online at https://doi.org/10.1016/j.envpol.2018.12.075.

References

Bendersky, M., Davis, J.M., 2011. DLVO interaction of colloidal particles with topographically and chemically heterogeneous surfaces. J. Colloid Interface Sci. 353 (1), 87–97.
Bhattacharjee, S., Chunhan Ko, A., Elimelech, M., 1998. DLVO interaction between rough surfaces. Langmuir 14 (12), 3365–3375.
Bozgeyik, K., Kopac, T., 2016. Adsorption properties of arc produced multi walled carbon nanotubes for bovine serum albumin. Int. J. Chem. React. Eng. 14 (2), 549–558.
Bradford, S.A., Kim, H., Shen, C., Sasidharan, S., Shang, J., 2017. Contributions of nanoscale roughness to anomalous colloid retention and stability behavior. Langmuir 33 (38), 10094–10105.
Bradford, S.A., Kim, H.N., Haznedaroglu, B.Z., Torkzaban, S., Walker, S.L., 2009. Coupled factors influencing concentration-dependent colloid transport and retention in saturated porous media. Environ. Sci. Technol. 43 (18), 6996–7002.
Bradford, S.A., Simunek, J., Bettahar, M., van Genuchten, M.T., Yates, S.R., 2006. Significance of straining in colloid deposition: evidence and implications. Water Resour. Res. 42 (12).
Bradford, S.A., Torkzaban, S., 2013. Colloid interaction energies for physically and chemically heterogeneous porous media. Langmuir 29 (11), 3668–3676.
Bradford, S.A., Torkzaban, S., 2015. Determining parameters and mechanisms of colloid retention and release. Langmuir ACS J. Surf. Colloids 31 (44), 12096–12105.
Bradford, S.A., Torkzaban, S., Walker, S.L., 2007. Coupling of physical and chemical mechanisms of colloid straining in saturated porous media. Water Res. 41 (13), 3012–3024.
Burdige, D.J., Kline, S.W., Chen, W., 2004. Fluorescent dissolved organic matter in marine sediment pore waters. Mar. Chem. 89 (1), 289–311.
Chen, M., Wang, D., Yang, F., Xu, X., Xu, N., Cao, X., 2017. Transport and retention of biochar nanoparticles in a paddy soil under environmentally-relevant solution chemistry conditions. Environ. Pollut. 230 (Suppl. C), 540–549.
Cheng, D., Liao, P., Yuan, S., 2016. Effects of ionic strength and cationic type on humic acid facilitated transport of tetracycline in porous media. Chem. Eng. J. 284, 389–394.
Dittmar, T., Paeng, J., Gihring, T.M., Suryaputra, I.G.N.A., Huettel, M., 2012. Discharge of dissolved black carbon from a fire-affected intertidal system. Limnol. Oceanogr. 57 (4), 1171–1181.
Dong, H., Ahmad, K., Zeng, G., Li, Z., Chen, G., He, Q., Xie, Y., Wu, Y., Zhao, F., Zeng, Y., 2016. Influence of fulvic acid on the colloidal stability and reactivity of nanoscale zero-valent iron. Environ. Pollut. 211, 363–369.
Espinasse, B., Hotze, E.M., Wiesner, M.R., 2007. Transport and retention of colloidal aggregates of C_{60} in porous media: effects of organic macromolecules, ionic composition, and preparation method. Environ. Sci. Technol. 41 (21), 7396–7402.
Fang, J., Xu, M.J., Wang, D.J., Wen, B., Han, J.Y., 2013. Modeling the transport of TiO2 nanoparticle aggregates in saturated and unsaturated granular media: effects of ionic strength and pH. Water Res. 47 (3), 1399–1408.
Franchi, A., O'Melia, C.R., 2003. Effects of natural organic matter and solution chemistry on the deposition and reentrainment of colloids in porous media. Environ. Sci. Technol. 37 (6), 1122–1129.
Furkan, M., Rizvi, A., Alam, M.T., Zaman, M., Khan, R.H., Naeem, A., 2017. Serotonin abrogates dopamine induced aggregation of cytochrome c. Int. J. Biol.

Macromol. 102, 893.
Furukawa, Y., Watkins, J.L., Kim, J., Curry, K.J., Bennett, R.H., 2009. Aggregation of montmorillonite and organic matter in aqueous media containing artificial seawater. Geochem. Trans. 10 (1), 2.
Guggenberger, G., Rodionov, A., Shibistova, O., Grabe, M., Kasansky, O.A., Fuchs, H., Mikheyeva, N., Zrazhevskaya, G., Flessa, H., 2008. Storage and mobility of black carbon in permafrost soils of the forest tundra ecotone in Northern Siberia. Global Change Biol. 14 (6), 1367–1381.
He, J., Li, C., Wang, D., Zhou, D., 2015. Biofilms and extracellular polymeric substances mediate the transport of graphene oxide nanoparticles in saturated porous media. J. Hazard Mater. 300, 467–474.
Hockaday, W.C., Grannas, A.M., Kim, S., Hatcher, P.G., 2007. The transformation and mobility of charcoal in a fire-impacted watershed. Geochem. Cosmochim. Acta 71 (14), 3432–3445.
Hoek, E.M., Agarwal, G.K., 2006. Extended DLVO interactions between spherical particles and rough surfaces. J. Colloid Interface Sci. 298 (1), 50–58.
Huang, X., Bhattacharjee, S., Hoek, E.M.V., 2010. Is surface roughness a "scapegoat" or a primary factor when defining Particle–Substrate interactions? Langmuir 26 (4), 2528.
Huangfu, X., Jiang, J., Ma, J., Liu, Y., Yang, J., 2013. Aggregation kinetics of manganese dioxide colloids in aqueous solution: influence of humic substances and biomacromolecules. Environ. Sci. Technol. 47 (18), 10285–10292.
Jones, E.H., Su, C., 2014. Transport and retention of zinc oxide nanoparticles in porous media: effects of natural organic matter versus natural organic ligands at circumneutral pH. J. Hazard Mater. 275, 79–88.
Jones, M.N., Bryan, N.D., 1998. Colloidal properties of humic substances. Adv. Colloid Interface 78 (1), 1–48.
Jung, B., O'Carroll, D., Sleep, B., 2014. The influence of humic acid and clay content on the transport of polymer-coated iron nanoparticles through sand. Sci. Total Environ. 496, 155–164.
Kim, H.N., Bradford, S.A., Walker, S.L., 2009. Escherichia coil O157:H7 transport in saturated porous media: role of solution chemistry and surface macromolecules. Environ. Sci. Technol. 43 (12), 4340–4347.
Kretzschmar, R., Robarge, W.P., Amoozegar, A., 1995. Influence of natural organic-matter on colloid transport through saprolite. Water Resour. Res. 31 (3), 435–445.
Lehmann, J., 2007a. Bio-energy in the black. Front. Ecol. Environ. 5 (7), 381–387.
Lehmann, J., 2007b. A handful of carbon. Nature 447 (7141), 143–144.
Lehmann, J., Gaunt, J., Rondon, M., 2006. Bio-char sequestration in terrestrial ecosystems – a review. Mitig. Adapt. Strat. Gl. 11 (2), 395–419.
Lehmann, J., Joseph, S., 2015. Biochar for environmental management: science, technology and implementation. Sci. Technol. Earthscan 25 (1), 15801–15811, 15811.
Lehmann, J., Rillig, M.C., Thies, J., Masiello, C.A., Hockaday, W.C., Crowley, D., 2011. Biochar effects on soil biota – a review. Soil Biol. Biochem. 43 (9), 1812–1836.
Liang, Y., Bradford, S.A., Simunek, J., Vereecken, H., Klumpp, E., 2013. Sensitivity of the transport and retention of stabilized silver nanoparticles to physicochemical factors. Water Res. 47 (7), 2572–2582.
Lin, D., Story, S.D., Walker, S.L., Huang, Q., Liang, W., Cai, P., 2017. Role of pH and ionic strength in the aggregation of TiO_2 nanoparticles in the presence of extracellular polymeric substances from Bacillus subtilis. Environ. Pollut. 228, 35–42.
Liu, Y., Yang, C.-H., Li, J., 2007. Influence of extracellular polymeric substances on Pseudomonas aeruginosa transport and deposition profiles in porous media. Environ. Sci. Technol. 41 (1), 198–205.
McKeon, K., Love, B., 2008. The presence of adsorbed proteins on particles increases aggregated particle sedimentation, as measured by a light scattering technique. J. Adhesion 84 (7), 664–674.
Mohd Omar, F., Abdul Aziz, H., Stoll, S., 2014. Aggregation and disaggregation of ZnO nanoparticles: influence of pH and adsorption of Suwannee River humic acid. Sci. Total Environ. 468–469, 195–201.
Morales, V.L., Zhang, W., Gao, B., Lion, L.W., Bisogni Jr., J.J., McDonough, B.A., Steenhuis, T.S., 2011. Impact of dissolved organic matter on colloid transport in the vadose zone: deterministic approximation of transport deposition coefficients from polymeric coating characteristics. Water Res. 45 (4), 1691–1701.
More, T.T., Yadav, J.S.S., Yan, S., Tyagi, R.D., Surampalli, R.Y., 2014. Extracellular polymeric substances of bacteria and their potential environmental applications. J. Environ. Manage. 144 (Suppl. C), 1–25.
Nakamura, M., Ohshima, H., Kondo, T., 1992. Electrophoretic behavior of antigen- and antibody-carrying latex particles. J. Colloid Interface Sci. 149 (1), 241–246.
Narvekar, S.P., Ritschel, T., Totsche, K.U., 2017. Colloidal stability and mobility of extracellular polymeric substance amended hematite nanoparticles. Vadose Zone J. 16 (8).
Nebbioso, A., Piccolo, A., 2013. Molecular characterization of dissolved organic matter (DOM): a critical review. Anal. Bioanal. Chem. 405 (1), 109–124.
Obia, A., Borresen, T., Martinsen, V., Cornelissen, G., Mulder, J., 2017. Vertical and lateral transport of biochar in light-textured tropical soils. Soil Till. Res. 165, 34–40.
Ohshima, H., Nakamura, M., Kondo, T., 1992. Electrophoretic mobility of colloidal particles coated with a layer of adsorbed polymers. Colloid Polym. Sci. 270 (9), 873–877.
Palomino, D., Stoll, S., 2013. Fulvic acids concentration and pH influence on the stability of hematite nanoparticles in aquatic systems. J. Nanoparticle Res. 15 (2), 1528.
Phenrat, T., Song, J.E., Cisneros, C.M., Schoenfelder, D.P., Tilton, R.D., Lowry, G.V., 2010. Estimating attachment of nano- and submicrometer-particles coated with organic macromolecules in porous media: development of an empirical model. Environ. Sci. Technol. 44 (12), 4531–4538.
Philippe, A., Schaumann, G.E., 2014. Interactions of dissolved organic matter with natural and engineered inorganic colloids: a review. Environ. Sci. Technol. 48 (16), 8946–8962.
Piccolo, A., 2001. The supramolecular structure of humic substances. Soil Sci. 166 (11), 810–832.
Qian, L., Zhang, W., Yan, J., Han, L., Gao, W., Liu, R., Chen, M., 2016. Effective removal of heavy metal by biochar colloids under different pyrolysis temperatures. Bioresour. Technol. 206, 217–224.
Rahman, T., Millwater, H., Shipley, H.J., 2014. Modeling and sensitivity analysis on the transport of aluminum oxide nanoparticles in saturated sand: effects of ionic strength, flow rate, and nanoparticle concentration. Sci. Total Environ. 499, 402–412.
Rijnaarts, H.H.M., Norde, W., Lyklema, J., Zehnder, A.J.B., 1999. DLVO and steric contributions to bacterial deposition in media of different ionic strengths. Colloids Surf. B Biointerf. 14 (1–4), 179–195.
Salgin, S., Salgin, U., Bahadır, S., 2012. Zeta potentials and isoelectric points of biomolecules: the effects of ion types and ionic strengths. Int. J. Electrochem. Sci. 7 (12), 12404.
Shang, J.Y., Liu, C.X., Wang, Z.M., Wu, H., Zhu, K.K., Li, J.A., Liu, J., 2010. In-situ measurements of engineered nanoporous particle transport in saturated porous media. Environ. Sci. Technol. 44 (21), 8190–8195.
Shen, M.H., Yin, Y.G., Booth, A., Liu, J.F., 2015. Effects of molecular weight-dependent physicochemical heterogeneity of natural organic matter on the aggregation of fullerene nanoparticles in mono- and di-valent electrolyte solutions. Water Res. 71, 11–20.
Sheng, A., Liu, F., Xie, N., Liu, J., 2016. Impact of proteins on aggregation kinetics and adsorption ability of hematite nanoparticles in aqueous dispersions. Environ. Sci. Technol. 50 (5), 2228–2235.
Šimunek, J., Šejna, M., van Genuchten, M.T., 1998. The HYDRUS-1D Software Package for Simulating the One-dimensional Movement of Water, Heat, and Multiple Solutes in Variably-saturated Media. IGWMC-TPS-70, Version 2.0.
Sun, P.D., Shijirbaatar, A., Fang, J., Owens, G., Lin, D.H., Zhang, K.K., 2015. Distinguishable transport behavior of zinc oxide nanoparticles in silica sand and soil columns. Sci. Total Environ. 505, 189–198.
Sun, W., Zhang, C., Shi, W., Wang, C., Jiao, X., 2016. Heteroadsorption of 17α-ethynylestradiol by multi-walled carbon nanotubes and SiO_2/Al_2O_3 nanoparticles: effect of surface-coated fulvic acid and alginate. Chem. Eng. J. 288, 516–524.
Suresh, L., Walz, J.Y., 1996. Effect of surface roughness on the interaction energy between a colloidal sphere and a flat plate. J. Colloid Interface Sci. 183 (1), 199–213.
Tian, R., Yang, G., Liu, X., Huang, C., Gao, X., Li, H., 2015. Observation of the unusual aggregation kinetics of colloidal minerals in acidic solutions. J. Chem. Sci. 127 (6), 1083–1089.
Torkzaban, S., Bradford, S.A., 2016. Critical role of surface roughness on colloid retention and release in porous media. Water Res. 88, 274–284.
Torkzaban, S., Tazehkand, S.S., Walker, S.L., Bradford, S.A., 2008. Transport and fate of bacteria in porous media: coupled effects of chemical conditions and pore space geometry. Water Resour. Res. 44 (4), 159–172.
Treumann, S., Torkzaban, S., Bradford, S.A., Visalakshan, R.M., Page, D., 2014. An explanation for differences in the process of colloid adsorption in batch and column studies. J. Contam. Hydrol. 164, 219–229.
Vaidyanathan, R., Chi, T., 1991. Hydrosol deposition in granular media under unfavorable surface conditions. Chem. Eng. Sci. 46 (4), 967–983.
Wang, D., Jaisi, D.P., Yan, J., Jin, Y., Zhou, D., 2015. Transport and retention of polyvinylpyrrolidone-coated silver nanoparticles in natural soils. Vadose Zone J. 14 (7).
Wang, D., Zhang, W., Hao, X., Zhou, D., 2013a. Transport of biochar particles in saturated granular media: effects of pyrolysis temperature and particle size. Environ. Sci. Technol. 47 (2), 821–828.
Wang, D., Zhang, W., Zhou, D., 2013b. Antagonistic effects of humic acid and iron oxyhydroxide grain-coating on biochar nanoparticle transport in saturated sand. Environ. Sci. Technol. 47 (10), 5154–5161.
Wu, D., He, L., Ge, Z., Tong, M., Kim, H., 2018. Different electrically charged proteins result in diverse bacterial transport behaviors in porous media. Water Res. 143, 425–435.
Xia, T., Fortner, J.D., Zhu, D., Qi, Z., Chen, W., 2015. Transport of sulfide-reduced graphene oxide in saturated quartz sand: cation-dependent retention mechanisms. Environ. Sci. Technol. 49 (19), 11468–11475.
Xiao, Y., Wiesner, M.R., 2013. Transport and retention of selected engineered nanoparticles by porous media in the presence of a biofilm. Environ. Sci. Technol. 47 (5), 2246–2253.
Yang, H., Kim, H., Tong, M., 2012a. Influence of humic acid on the transport behavior of bacteria in quartz sand. Colloids Surf. B Biointerf. 91, 122–129.
Yang, J., Bitter, J.L., Smith, B.A., Fairbrother, D.H., Ball, W.P., 2013. Transport of oxidized multi-walled carbon nanotubes through silica based porous media: influences of aquatic chemistry, surface chemistry, and natural organic matter. Environ. Sci. Technol. 47 (24), 14034–14043.
Yang, W., Wang, Y., Shang, J., Liu, K., Sharma, P., Liu, J., Li, B., 2017a. Antagonistic effect of humic acid and naphthalene on biochar colloid transport in saturated porous media. Chemosphere 189, 556–564.
Yang, W., Wang, Y., Sharma, P., Li, B., Liu, K., Liu, J., Flury, M., Shang, J., 2017b. Effect of naphthalene on transport and retention of biochar colloids through saturated porous media. Colloids Surf. A Physicochem. Eng. Asp. 530, 146–154.

Yang, X., Deng, S., Chen, F., Flynn, R., von der Kammer, F., Hofmann, T., 2012b. Comparing the influence of two different natural organic matter types on colloid deposition in saturated porous medium. Adv. Mater. Res. 455–456, 1324–1329.

Yavari, S., Malakahmad, A., Sapari, N.B., 2015. Biochar efficiency in pesticides sorption as a function of production variables-a review. Environ. Sci. Pollut. Res. 22 (18), 13824–13841.

Yuan, B., Pham, M., Nguyen, T.H., 2008. Deposition kinetics of bacteriophage MS2 on a silica surface coated with natural organic matter in a radial stagnation point flow cell. Environ. Sci. Technol. 42 (20), 7628–7633.

Zhang, M., Bradford, S.A., Simunek, J., Vereecken, H., Klumpp, E., 2016. Do goethite surfaces really control the transport and retention of multi-walled carbon nanotubes in chemically heterogeneous porous media? Environ. Sci. Technol. 50 (23), 12713–12721.

Zhang, W., Niu, J., Morales, V.L., Chen, X., Hay, A.G., Lehmann, J., Steenhuis, T.S., 2010. Transport and retention of biochar particles in porous media: effect of pH, ionic strength, and particle size. Ecohydrology 3 (4), 497–508.

Zhang, W., Rattanaudompol, U.S., Li, H., Bouchard, D., 2013. Effects of humic and fulvic acids on aggregation of aqu/nC_{60} nanoparticles. Water Res. 47 (5), 1793–1802.